Cell Stress and Chaperones (2024) 29:721–734
https://doi.org/10.1016/j.cstres.2024.10.004

Functional similarities and differences among subunits of the nascent polypeptide-associated complex (NAC) of *Saccharomyces cerevisiae*

Brenda A. Schilke[1] · Thomas Ziegelhoffer[1] · Przemyslaw Domanski[2,3] · Jaroslaw Marszalek[2] · Bartlomiej Tomiczek[2] · Elizabeth A. Craig[1,*]

Received: 16 September 2024 / Revised: 11 October 2024 / Accepted: 15 October 2024

Abstract

Protein factors bind ribosomes near the tunnel exit, facilitating protein trafficking and folding. In eukaryotes, the heterodimeric nascent polypeptide-associated complex (NAC) is the most abundant—equimolar to ribosomes. *Saccharomyces cerevisiae* has a minor β-type subunit (Nacβ2) in addition to abundant Nacβ1, and therefore two NAC heterodimers, α/β1 and α/β12. The additional beta NAC gene arose at the time of the whole genome duplication that occurred in the *S. cerevisiae* lineage. Nacβ2 has been implicated in regulating the fate of messenger RNA encoding ribosomal protein Rpl4 during translation *via* its interaction with the Caf130 subunit of the regulatory CCR4-Not complex. We found that Nacβ2 residues just C-terminal to the globular domain are required for its interaction with Caf130 and its negative effect on the growth of cells lacking Acl4, the specialized chaperone for Rpl4. Substitution of these Nacβ2 residues at homologous positions in Nacβ1 results in a chimeric protein that interacts with Caf130 and slows the growth of Δ*acl4* cells lacking Nacβ2. Furthermore, alteration of residues in the N-terminus of Nacβ2 or chimeric Nacβ1 previously shown to affect ribosome binding overcomes the growth defect of Δ*acl4*. Our results are consistent with a model in which Nacβ2's ribosome association *per se* or its precise positioning is necessary for productive recruitment of CCR4-Not *via* its interaction with the Caf130 subunit to drive Rpl4 messenger RNA degradation.

Keywords Ribosomal chaperones · Protein biogenesis factors · Postduplication protein divergence · Protein evolution · NAC-ribosome interaction · CCR4-Not1 complex

Introduction

A number of protein biogenesis factors bind to ribosomes at the tunnel exit, in close proximity to emerging nascent polypeptide chains. The most abundant is the nascent chain-associated complex (NAC). *In vivo* and *in vitro* results, mainly using metazoan systems, indicate that NAC plays important roles in "directing" nascent chains to the appropriate cellular location—by blocking or providing access to factors such as signal recognition particle or methionine aminopeptidases.[1–3] NAC also has molecular chaperone activity, for example, preventing aggregation of polypeptide chains.[4] NAC contains two distantly related subunits, alpha and beta,[5,6] both of which are less than 20 kDa (Figure 1(a)). Internal segments form the globular core of the α/β heterodimer, which includes antiparallel N-terminal helices followed by 5 beta strands of each subunit. Both subunits also have N-terminal and C-terminal extensions. The N-terminus of the beta subunit is important for NAC's association with the ribosome, through the interaction of positively charged residues with ribosomal RNA (rRNA).[7,8]

Three genes in the *Saccharomyces cerevisiae* genome encode NAC subunits[9,10] (Figure 1(a)): *EGD2*, the Nacα subunit; *EGD1,* the abundant Nacβ1 subunit; *BTT1*, the minor Nacβ2 subunit. Nacα and Nacβ1 subunits are at least as abundant as ribosomes, while Nacβ2 is on the order of 20–100 fold less abundant.[11] In some

* Elizabeth A. Craig
ecraig@wisc.edu

[1] Department of Biochemistry, University of Wisconsin-Madison, Madison, WI 53726, United States

[2] Intercollegiate Faculty of Biotechnology, University of Gdansk, Gdansk, Poland

[3] Department of Physical Chemistry, Gdansk University of Technology, Gdansk, Poland.

Published online: 18 October 2024

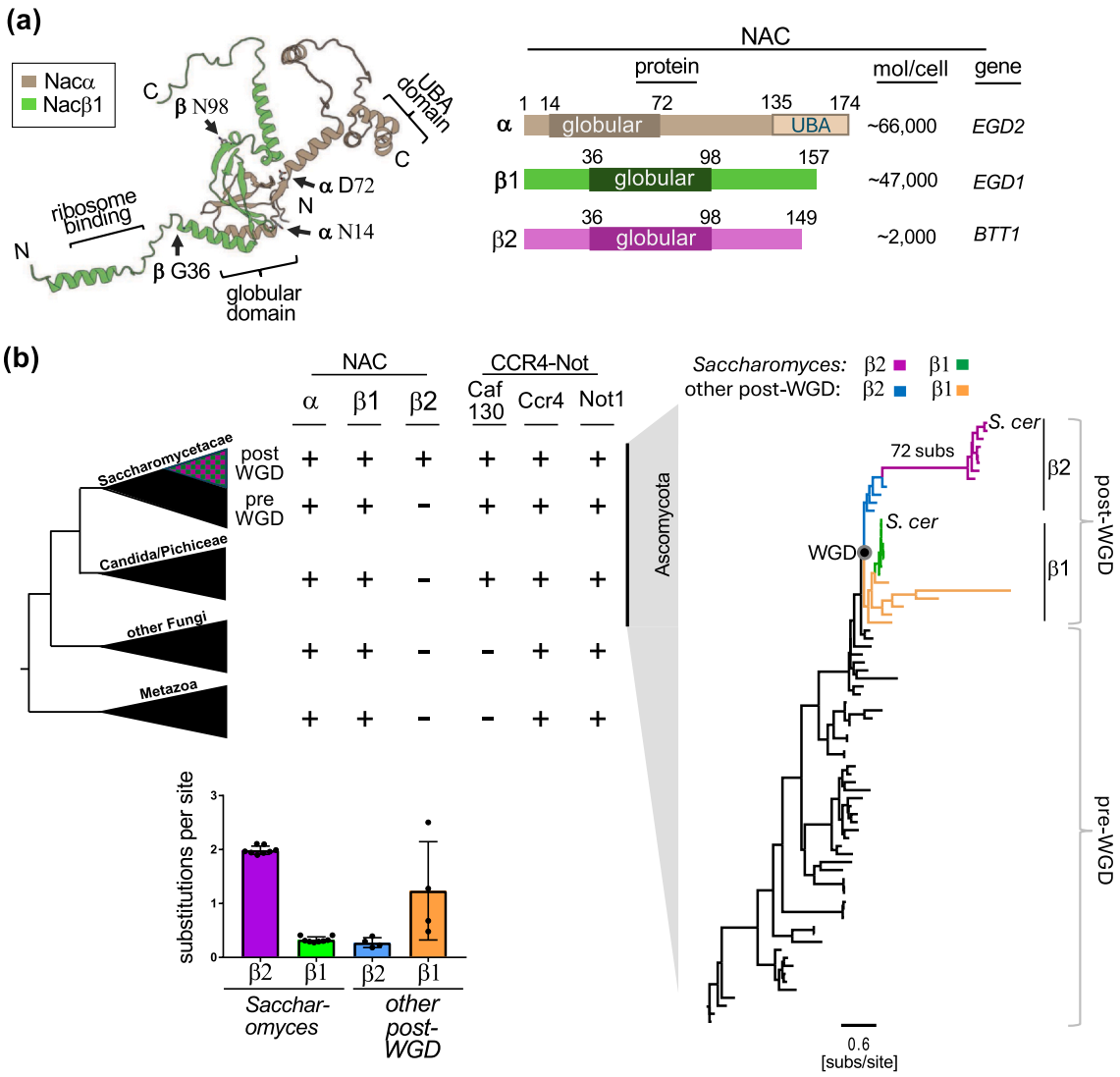

Fig. 1 Evolution of Nacβ1 and Nacβ2 (a) left. Structural model of Nacα/Nacβ1 heterodimer (10.5452/ma-bak-cepc-0495); Nacα (brown); Nacβ1 (green). The bracket designates the globular domain, with its beginning and end indicated by arrows and residue for each subunit. Right. Summary of NAC subunits of *Saccharomyces cerevisiae* with line diagram indicating the globular domains and presence of the UBA domain at the C-terminus of Nacα. Gene names and estimated number of molecules per cell also indicated. (b) Top left. Taxonomic distribution of NAC subunits and selected components of CCR4–Not complex. Saccharomycetacae pre-WGD and post-WGD clades are indicated. Right: Nacβ protein family evolution in Ascomycota. Phylogeny was reconstructed using beta NAC homologs from 9 pre-WGD and 13 post-WGD Saccharomycetacae species and 41 homologs from other Ascomycota species using maximum likelihood. The tree topology was constrained such that post-WGD sequences share common ancestry at the WGD node. Nacβ2 (β2): *Saccharomyces* (magenta); other post-WGD species (blue). Nacβ1 (β1): *Saccharomyces* (green); other post-WGD species (orange). Nacβ1 and Nacβ2 from *S. cerevisiae* are indicated. Scale bar—amino acid substitutions per site. Bottom left. Evolutionary distance (substitutions per site) calculated along the branches of the phylogenetic tree from the WGD node to the tips representing beta NAC sequences from post-WGD species. Saccharomyces Nacβ2 (magenta) and Saccharomyces Nacβ1 (green); other post-WGD Nacβ2 (blue) and other post-WGD Nacβ1 (orange). Abbreviations used: UBA, ubiquitin-associated; WGD, whole genome duplication.

metazoans, NAC has been shown to be essential.[12] In fungi it is not, though its absence causes temperature-sensitive growth in some *S. cerevisiae* strain backgrounds.[10,13] This lack of essentiality in fungi has been attributed in part to the presence in fungi of the specialized ribosome-associated Hsp70 Ssb.[14] Ssb is the Hsp70 partner of the specialized ribosome-associated J-domain protein Zuotin found in all eukaryotes. But in plants and metazoans, Zuotin functions with the general cytosolic Hsp70s. Ssb and Zuotin are in very close proximity to NAC at the ribosome tunnel exit, as both can be crosslinked to NAC on the ribosome.[15]

Nacβ2, but not Nacβ1, has been implicated in the regulation of the amount of ribosomal protein Rpl4 synthesized.[16] On the practical side, this regulation allows a simple, sensitive readout of Nacβ2 function as its absence allows robust growth of cells having a deletion of the Rpl4-specific chaperone Acl4, which in an otherwise WT background grows very slowly.[17,18] However, this effect is the result of the action of a conserved complex regulatory system, CCR4–Not, which is involved in global regulation of messenger RNA (mRNA) metabolism both on and off the ribosome.[19–21] Acl4 chaperone activity is critical because Rpl4 is aggregation-prone when not incorporated into ribosomes.[22] When Acl4 is absent or limiting, ribosome-associated Rpl4 mRNA is degraded *via* CCR4–Not, preventing the accumulation of aggregated Rpl4.[16] Evidence indicates that this regulation depends on the recently detected interaction of Nacβ2 (but not Nacβ1) with the Caf130 component of the CCR4–Not complex.[16,23] The absence of either Nacβ2 or Caf130 suppresses the growth defect of cells lacking Acl4 by alleviating the tight control of mRNA levels.[16] This relief of tight control is thought to allow sufficient expression of Rpl4 to allow more ribosome production, which in turn permits robust growth.

Here, we report the results of our analysis of the specificities and similarities of the two *S. cerevisiae* beta NAC subunits. We found that minimal substitutions outside the globular domain of Nacβ2 disrupt interaction with Caf130 and significantly overcome the growth defect of cells lacking Acl4.

Results and discussion

Evolution of beta NAC subunits and Caf130

As a first step to better understand differences between the two Nacβ subunits, we analyzed the evolution of the genes encoding Nacβ1 and Nacβ2. Caf130 was also analyzed because although a CCR4–Not complex is found across both fungi and metazoan species, the CCR4–Not-associated proteins vary among eukaryotes. Interestingly, the presence of both Caf130 and Nacβ2 is restricted to subsets of fungi species. Caf130 is present in the Saccharomycotina clade (Figure 1(b)) but absent in other fungi and in metazoans. Nacβ2 has an even more limited distribution—present in a subset of yeast species that underwent a whole genome duplication (WGD) event.[24] Such a distribution suggests that Nacβ2 emerged during the WGD and belongs to a relatively small group of ~450 genes, for which two duplicates were maintained in post-WGD lineages.[25]

We identified Nacβ1 and Nacβ2 orthologs in post-WGD species based on their position in the genome (i.e., synteny). Among the 13 post-WGD species analyzed, 11 have both Nacβ1 and Nacβ2, while 2 have only Nacβ2. To further analyze the evolutionary relationships among Nacβ1 and Nacβ2 proteins, we reconstructed their phylogeny using the maximum likelihood method (Figures 1(b) and S1). Nacβ2 sequences from *S. cerevisiae* and closely related species (genus Saccharomyces) stand out (Figure 1(b), purple). They form a monophyletic group with a very long stem branch, signifying that shared amino acid substitutions accumulated in this lineage—an indication of rapid postduplication divergence. In stark contrast, as indicated by their short branches, paralogous Nacβ1 sequences from the same Saccharomyces species accumulated only a few substitutions (Figure 1(b), green). Calculating the number of substitutions along the branches of the tree for Nacβ2 and Nacβ1 sequences from Saccharomyces (Figure 1(b)) revealed, on average, six-fold more substitutions for Nacβ2 than for Nacβ1. This substantial accumulation of substitutions in Nacβ2 did not occur in other post-WGD species—in fact, Nacβ1 sequences accumulated on average more substitutions than Nacβ2 (Figure 1(b)). It is also worth noting that, in contrast to other post-WGD species, all analyzed Saccharomyces species maintained both Nacβ1 and Nacβ2.

For this report focusing on *S. cerevisiae*, the important point is that our analysis revealed that, in the Saccharomyces lineage, Nacβ2 evolved rapidly, accumulating many substitutions, while Nacβ1 evolved slowly, preserving much of its pre-WGD sequence. It is often the case that one duplicate (i.e., Nacβ1) maintains both the original preduplication function(s) and expression level, while the other duplicate (i.e., Nacβ2) evolves a new function and reduced expression level.[26–30] It is also well documented that a lower expression level correlates with a higher accumulation of neutral and near-neutral substitutions.[31–33] However, this makes it challenging to tease out sequence differences responsible for functional differences. As discussed below, we turned to a genetic approach to better define the sequences in Nacβ2 specifically important for its function in relation to Acl4 and whether other aspects of NAC functionality held in common with Nacβ1 are important as well.

A Nacβ2 segment C-terminal to the globular domain is required to exacerbate Δ*acl4* growth defect

To better define sequences in Nacβ2 required for inhibition of growth of cells lacking Acl4, we made constructs to express variants, concentrating on the regions least conserved between it and Nacβ1 (Figure 2(a)). We first tested a 7 residue segment that is just N-terminal to the α-helix of the globular domain, spanning residues 31–37 (^{31}GNLYNNN^{37}). This segment of Nacβ2 was replaced by the analogous segment of Nacβ1 (^{31}AGSSAGA^{37}), generating Nacβ2(β1$_{31–37}$). Δ*acl4* Δ*nac*β2 cells expressing Nacβ2(β1$_{31–37}$) grew as poorly as those expressing wild-type (WT) Nacβ2 (Figure 2(c)), indicating that it maintained Nacβ2-specific activity. Next, we made Nacβ2 C-terminal truncations as there is little sequence identity between Nacβ1 and Nacβ2 in this region (Figure 2(b)). Δ*acl4* Δ*nac*β2 cells expressing Nacβ2$_{1–126}$, which lacks the 23 most C-terminal residues, grew as poorly as cells expressing full-length Nacβ2. But those expressing Nacβ2$_{1–111}$ grew well (Figure 2(c)), suggesting a loss of Nacβ2 regulatory function and implicating residues between 112 and 126 as functionally important.

To better define important residues, we made two NACβ2 variants based on comparison with Nacβ1 sequences (Figure 2(a)), beginning with substituting[1]: all Nacβ2 residues for those of Nacβ1 between positions 112 and 117 (i.e., ^{112}SQELEY^{117} to ^{112}PEAIQA^{117})[2]; residues at positions 120, 123, and 124 (G120Q/H123A/N124Q). The variant with substitutions within the 112–117 interval suppressed the Δ*acl4* growth defect, indicating loss of

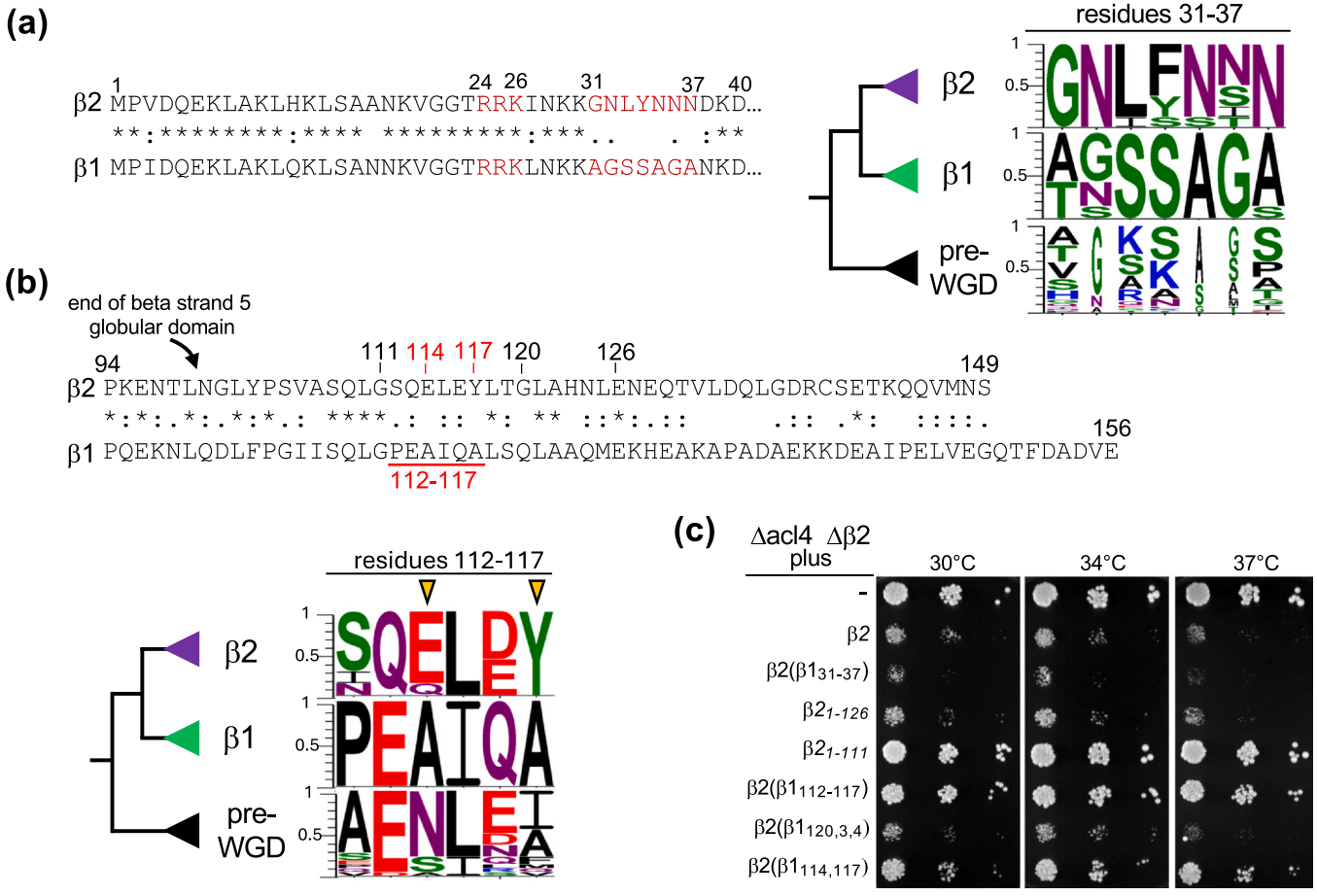

Fig. 2 Sequences C-terminal to the globular domain of Nacβ2 important in inhibiting the growth of cells lacking Acl4. Sequences comparisons of segments N-terminal (a) and C-terminal (b) to the globular domains of Nacβ2 and Nacβ1 ("*" invariant, ":" high similarity, "." low similarity). Sequence particularly relevant for genetic analyses underlined/highlighted in red, including RRK (residues 24–26) previously demonstrated to be important for interaction with the ribosome. Sequence logos represent the amino acid frequency of each residue position in the 31–37 and 112–117 segments of Nacβ1 (β1) and Nacβ2 (β2) post-WGD, and for Nacβ1 pre-WGD (pre-WGD): positively charged (blue), negatively charged (red), neutral (purple), polar (green), hydrophobic (black); narrow lettering indicates the presence of gaps in the alignment. Position numbering for *S. cerevisiae*. Position of single residue changes made in the 112–117 segment indicated by arrowheads. (c) Ten-fold serial dilutions of Δ*acl4* Δ*nac*β2 (Δacl4 Δβ2) cells expressing the indicated Nacβ2 proteins from a plasmid (-, empty vector) were spotted onto plates and incubated at the indicated temperatures for 2 days. Abbreviation used: WGD, whole genome duplication

function. However, the 120/123/124 variant maintained function, that is, Δ*acl4* Δ*nac*β2 cells grew as poorly as when WT Nacβ2 was present. Based on conservation in the 112–117 region (Figure 2(b)), we then switched residues at positions 114 and 117 (E114A/Y117A). This double substitution variant has reduced function in regard to Δ*acl4*, that is, cells having the *ACL4* deletion grew better when expressing Nacβ2$_{E114A/Y117A}$ than when expressing WT Nacβ2 (Figure 2(c)).

The simplest explanation for the observed functional difference between WT Nacβ2 and the variants is a disruption of its interaction with Caf130. Since results of previous yeast two-hybrid assays defined a region between Nacβ2 residues 38 and 129 as sufficient for interaction with Caf130,[16] we decided to also employ yeast 2-hybrid assay analysis, which allows *in vivo* detection of protein-protein interaction, to test this idea (Figure 3(a)). As expected, cells grew well under 2-hybrid test conditions when WT Nacβ2 or Nacβ2$_{1–129}$ was used as bait. But when Nacβ1 or Nacβ2$_{1–111}$ was used, growth was not observed. Importantly, cells expressing Nacβ2$_{E114A/Y117A}$ also did not grow under test conditions, indicating that the substitutions that suppressed the Δ*acl4* growth defect also disrupted Nacβ2 interaction with Caf130. These results are consistent with the Caf130-Acl4 interaction being a key distinction between Nacβ1 and Nacβ2 in this function.

Because residues critical for the functional interaction with Caf130 (i.e., E114/Y117) are conserved among Nacβ2 sequences from Saccharomyces species (Figure 2(b)), we hypothesized that they emerged in their common ancestor. Indeed, phylogeny-based statistical reconstruction of the ancestral Nacβ2 sequences revealed that A114E/A117Y substitutions were among the 72 amino acid changes that took place along the long branch leading to the most recent common ancestor of Saccharomyces (Figure S1). What triggered the rapid divergence of the Nacβ2 sequence is unclear. However, many of these substitutions may be neutral, as no growth phenotypes were observed when the Nacβ2 regions encompassing them were swapped or deleted. These results are consistent with an evolutionary scenario where Nacβ2 appeared early as a result of the WGD, while substitutions critical for interaction with Caf130 emerged later, in the common ancestor of Saccharomyces. Therefore, these substitutions are only present in a subset of post-WGD species closely related to *S. cerevisiae*.

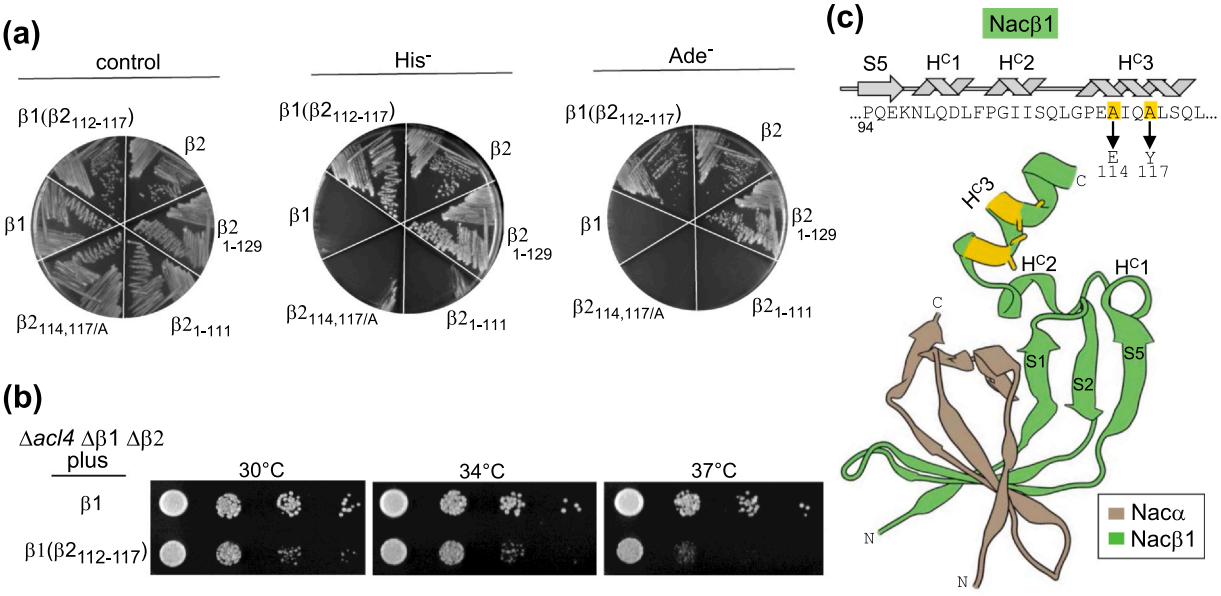

Fig. 3 Nacβ1/Nacβ2 interaction with Caf130. (a) Two-hybrid interaction of Nacβ1 and Nacβ2. Plasmids expressing full-length Caf130 fused to the *GAL4* activation domain and the indicated beta NAC wild-type or variants fused to the *GAL4* DNA binding domain were cotransformed into the 2-hybrid readout *S. cerevisiae* strain. Transformants were streaked on media selecting for the plasmids (left), or on media additionally lacking histidine (His, center) or adenine (Ade, right) and incubated at 30 °C for 3 days to monitor interaction. (b) Effect of Nacβ1 chimera on Δ*acl4* phenotype. Ten-fold serial dilutions of Δ*acl4* Δnacβ1 Δ*nac*β2 (Δacl4 Δβ1 Δβ2) cells expressing the indicated flag-tagged proteins were plated and grown for 2 days at indicated temperatures. (c) Model of NAC α/β1 heterodimer as in Figure 1(a) showing residues Nacα$^{29–73}$ Nacβ1 (53–121). Alanines at positions 114/117 in stick representation (yellow). Sequence shown above with beta strands 1, 2, 5 (S1, S2, S5) of globular domain and helical regions[1–3] of C-terminal extension (H^C1, H^C2, H^C3) indicated.

Substitution of Nacβ2 sequences in Nacβ1 confer Caf130 interaction and inhibition of Δ*acl4* growth

Since the results reported above are consistent with the idea that interaction with Caf130 is the sole functional difference between Nacβ2 and Nacβ1 in regard to regulation of Rpl4 levels, we wanted to ask if Nacβ1 could be "converted" to have Nacβ2-like function. We carried out two experiments analogous to those discussed above. First, residues at positions 112–117 of Nacβ1 were changed to those of Nacβ2 (^{112}PEAIQA^{117} to ^{112}SQELEY^{117}) generating Nacβ1(β2$_{112–117}$). Nacβ1(β2$_{112–117}$) supported growth under both 2-hybrid test conditions (Figure 3(a)), indicating interaction with Caf130. Next, we swapped this Nacβ2 segment into Nacβ1 for expression in yeast to test its effect on the growth of cells having a deletion of *ACL4*. Cells lacking Acl4, Nacβ1, and Nacβ2, but expressing Nacβ1(β2$_{112–117}$), grew more poorly than cells expressing WT Nacβ1, indicating that it had gained Nacβ2 activity (Figure 3(b)). Together, these results support the idea that the ability to interact with Caf130 is the sole difference between NACβ2 and NACβ1 needed to exert the "Nacβ2 negative effect" on Δ*acl4* growth.

As shown by initial crystal structures of human NAC[5,6] and structural modeling of yeast NAC,[34] an alpha-helical segment is immediately C-terminal to the last beta-strand of the globular domain (S5). This region is composed of two very short helical segments (H^{c}1 and H^{c}2), followed by a longer one (H^{c}3) that was not included in the crystal structures. The residues identified here as important for Caf130 interaction (114/117) are in H^{c}3 (Figure 3(c)). Their packing against the NAC globular domain in the model makes it unlikely that they directly participate in intermolecular interaction with Caf130. However, the more bulky E114/Y117 residues of Nacβ2 may confer a small difference in positioning of H^{c}3 that could, without introducing major structural changes, effect changes in conformation that allow or enhance a functionally stable interaction with Caf130. This possibility is especially intriguing considering that their location on H^{C}3 positions them close to the pivot point of any rotation between H^{C}3 and the NAC globular domain.

However, since no structural information is available for Caf130, a more detailed analysis of a Nacβ2-Caf130 interaction is problematic. Yet, it is intriguing that even though several functions have been attributed to the globular domain extensions of NAC,[35–37] to our knowledge, this is the first time the junction between the globular domain and C-terminal extension has been linked to an *in vivo* function. It will be interesting to see in the future whether other functions will be uncovered for this region.

Disturbance of Nacβ2 ribosome association promotes the growth of Δ*acl4* cells

Both NAC and the CCR4–Not complex are known to function at the ribosome. To examine whether a defect in ribosome association affects the ability of Nacβ2 to exacerbate the growth defect of Δ*acl4* cells, we employed the commonly used variant having alanine substitutions of the conserved sequence previously shown to affect ribosome association—^{24}RRK^{267} (see Figure 1(a)). Δ*acl4* Δ*nac*β2 cells expressing Nacβ2$_{RRK/AAA}$ grew better than those expressing WT Nacβ2 (Figure 4(a)). We also tested the effect when only Acl4 was absent. Nacβ2$_{RRK/AAA}$ improved the growth of Δ*acl4* cells, even though WT Nacβ2 was present, as did low expression of chimeric Nacβ1$_{RRK/AAA}$(β2$_{112–117}$). As expected, Nacβ1$_{RRK/AAA}$ did not (Figure 4(a)). Together, these results indicate a dominant effect of the RRK/AAA mutation in a beta NAC protein that can interact with Caf130.

Together the results presented in these three sections suggest a model (Figure 4(b)) in which Nacβ2's role in modulating the amount of Rpl4 synthesized is recruitment of the CCR4–Not complex to ribosomes translating Rpl4 mRNA—*via* its interaction with the Caf130 subunit. Presumably, this places CCR4–Not subunits directly involved in mRNA deadenylation and degradation (such as Not2, Not3, and Not5) in close proximity to the mRNA.[16,38] If Nacβ2 (or chimeric Nacβ1) defective in ribosome association is present, CCR4–Not is titrated away from the ribosome, negating degradation and resulting in an increase in Rpl4 synthesis. This increase in Rpl4 allows the production of more ribosomes, allowing more robust growth.

Cells lacking both beta subunits are temperature-sensitive but rescued by RRK/AAA variant

We noted during our analysis of Acl4 that, consistent with previous results using strain W303,[10] cells lacking both beta subunits (Δ*nac*β1 Δ*nac*β2) are temperature sensitive. The double mutant grows poorly at both 34 and 37 °C (Figure 5(a)). The single deletion strains (i.e., Δ*nac*β or Δ*nac*β2) grow like WT. The robust growth phenotype of cells lacking highly expressed Nacβ1 suggests that only a low level of heterodimer is required, as Nacβ2 is not upregulated in the absence of Nacβ1 (Figure 5(a)). To test whether lower levels of Nacβ1, like Nacβ2, are sufficient for WT growth, we placed it under the control of the Nacβ2 promoter. Expression was substantially reduced, yet cells having this construct grew as well as cells expressing normal levels of Nacβ1 (Figure 5(b)). We conclude that W303 requires only a low level of a NAC

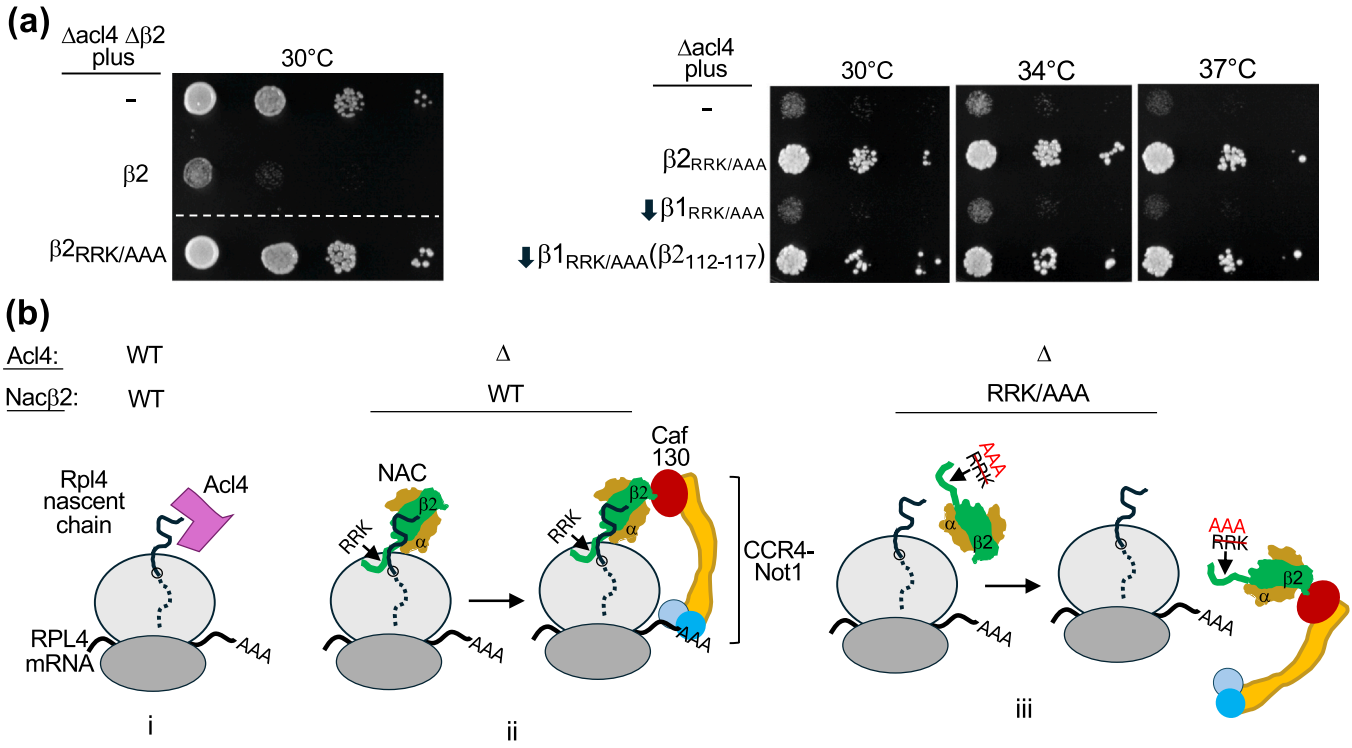

Fig. 4 Effect of RRK/AAA mutation on Δ*acl4* cells and model of function in absence of Acl4. (a) Ten-fold serial dilutions of Δ*acl4* Δ*nac*β2 (Δacl4 Δβ2) or Δacl4 cells (left and right, respectively) expressing the indicated Nacβ2, Nacβ1, or chimeric protein from a plasmid (↓ indicates wild type or chimeric Nacβ1 expressed from the Nacβ2 promoter; -, empty vector) were spotted onto plates and incubated at the indicated temperatures for 2 days. The dotted line on the left indicates splicing out of irrelevant strains from the image of the plate. (b) Model of the effect of NAC and the absence of Acl4 on the regulation of Rpl4 mRNA levels. (i) Normally, Acl4 binds Rpl4 nascent chains, preventing their aggregation. (ii) If Acl4 is absent, Nacα/Nacβ2 present near the tunnel exit of the 60S ribosomal subunit recruits CCR4–Not1 *via* interaction with its Caf130 subunit. Other subunits positioned near the mRNA on the 40S initiate the degradation of Rpl4 mRNA. (iii) If association of NAC with the ribosome is disturbed, CCR4–Not complex is not recruited to the ribosome (or positioned nonproductively), resulting in continued translation of mRNA, which allows assembly of sufficient ribosomes for robust growth. mRNA, messenger RNA.

heterodimer for normal growth, and either a Nacα/Nacβ1 or Nacα/Nacβ2 heterodimer suffices.

We next tested the ability of Nacβ2 having the RRK/AAA ribosome association mutation to overcome the temperature-sensitive growth phenotype of cells having neither WT Nacβ1 nor Nacβ2. Cells expressing either $Nac\beta1_{RRK/AAA}$ or $Nac\beta2_{RRK/AAA}$ as the only beta subunit grew as well as WT cells (Figure 5(c)), as did cells expressing $Nac\beta1_{RRK/AAA}$ under the control of the Nacβ2 promoter. This result was unexpected. As recent analyses have tied NAC function closely to the ribosome,[1,12,39,40] we had anticipated that the RRK/AAA variant would not support growth at 37 °C.

The standard test for ribosome association is comigration during high-speed centrifugation through a sucrose cushion to separate ribosomes from soluble proteins.[7,14] Such an assay requires sustained association after cell lysis. We therefore turned to *in vivo* site-specific crosslinking to assess the effect of the RRK to AAA substitution, because crosslinking prior to cell lysis could help stabilize the interaction through the sucrose cushion centrifugation step. Furthermore, this method provides an assessment of ribosome interaction in the cell. We made use of the previously detected ability of ribosome-associated Hsp70 Ssb1 to crosslink to NAC.[15] More specifically, Bpa, a photoactivatable non-canonical amino acid, when incorporated at position S563 of Ssb1, crosslinks to NACβ1 (Figure 5(d)). A crosslinked product between $Ssb1_{S563Bpa}$ and $Nac\beta1_{RRK/AAA}$ was also detected in the ribosome pellet fraction. Although less than that observed for WT Nacβ1, this result indicates that a portion of the RRK/AAA NAC variant is ribosome-associated in the cell.

The crosslinking results indicate that the RRK/AAA variant disturbs but does not completely disrupt NAC's ribosome association. Therefore, whether the temperature-sensitive phenotype of Δ*nac*β1 Δ*nac*β2 is due to a NAC function occurring on or off the ribosome remains unclear. Furthermore, it also leaves open the possibility that the effect of the RRK/AAA mutation on the Δ*acl4* phenotype could well be due to altered positioning of CCR4–Not at the ribosome rather than complete displacement from the ribosome. Furthermore, the crosslinked Ssb1–NAC we detected could be an underestimate,

as a change in the position of the globular domain could result in a decrease in crosslinking even though NAC is still present on the ribosome. Unfortunately, designing a variant that completely disrupts ribosome association without disrupting other functions as well is difficult. Other sequences in N-terminal regions,[8] as well as sequences in the helices of the globular domain,[41,42] have also been shown to affect NAC's binding to the ribosome.

In the presence or absence of Nacα, Nacβ2 supports growth as well as Nacβ1 when expressed similarly

To carry out the experiments described in the previous section, we constructed a strain carrying a deletion of the Nacα encoding gene. We noted that Δ*nac*α cells grew moderately slower at 37 °C than WT (Figure 6(a))—the only growth phenotype observed for a single NAC deletion.

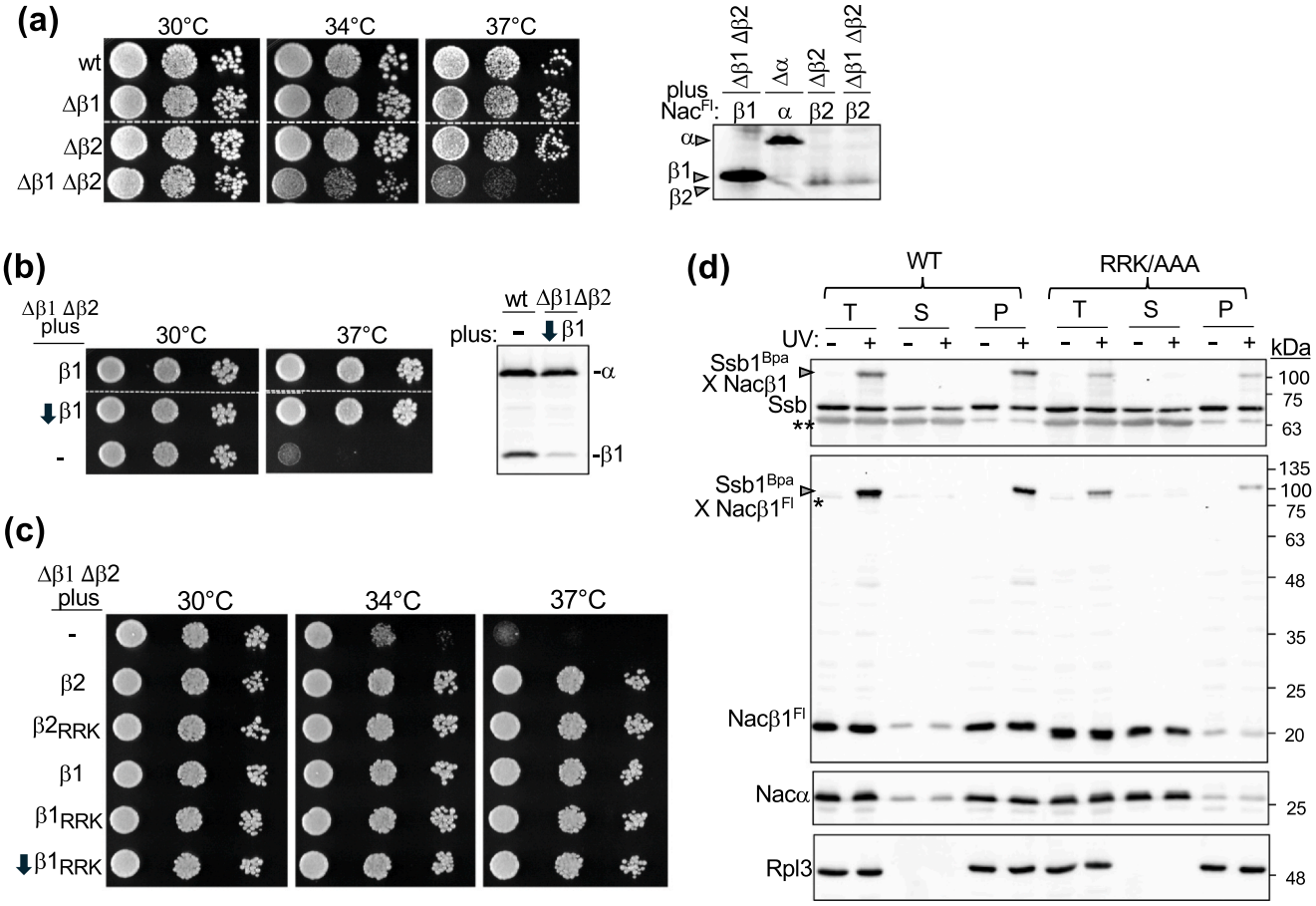

Fig. 5 Growth defect of cells lacking Nacβ1 and Nacβ2 and effect of RRK/AAA mutation. (a) Left. Growth of wild-type (WT) and strains having deletions of genes encoding beta NAC subunits: Nacβ1 (Δβ1), Nacβ2 (Δβ2), or both beta subunits (Δβ1 Δβ2). Ten-fold serial dilutions were plated on rich media and incubated at indicated temperatures for two days. The dotted line indicates the removal of nonrelevant strains from the plate image. Right. Indicated deletions were transformed with a plasmid carrying a gene encoding an NAC subunit with a Flag tag to allow comparison of expression levels. Immunoblot analysis of cell extracts separated by SDS-PAGE using antibody specific for the Flag tag. (b) Reduced expression of Nacβ1 by placement under the control of Nacβ2 promoter (↓β1). Left. Ten-fold serial dilutions of Δβ1 Δβ2 carrying indicated plasmid were plated and incubated for 2 days; empty vector (-). The three strains were plated on the same plate; the dotted line indicates the removal of nonrelevant strains from the plate image. Right. Immunoblot comparing levels of Nacα and Nacβ1 in wt cells and Δβ1 Δβ2 cells expressing Nacβ1 under control of Nacβ2 promoter. A mixture of polyclonal antibodies recognizing Nacα and Nacβ1 was used. (c) Growth of Δβ1 Δβ2 expressing RRK/AAA (RRK) variants. Ten-fold serial dilutions of Δβ1Δβ2 carrying indicated plasmid were plated and incubated at indicated temperatures for 2 days. (d) Immunoblot analysis of *in vivo* crosslinking on the ribosome between Ssb1 containing Bpa at position 563 and Flag-tagged Nacβ1 or $Nac\beta1_{RRK/AAA}$. After the separation of cell lysates *via* centrifugation through a sucrose cushion, samples of total, supernatant, and pellet were resolved on SDS-PAGE gels. UV-treated (+); untreated (-). Mobility of markers at right; Flag antibody was used to detect $Nac\beta1^{Fl}$; *, indicates background band that is present in total and supernatant fractions; **, truncated Ssb1 caused by incomplete incorporation of Bpa at stop codon.

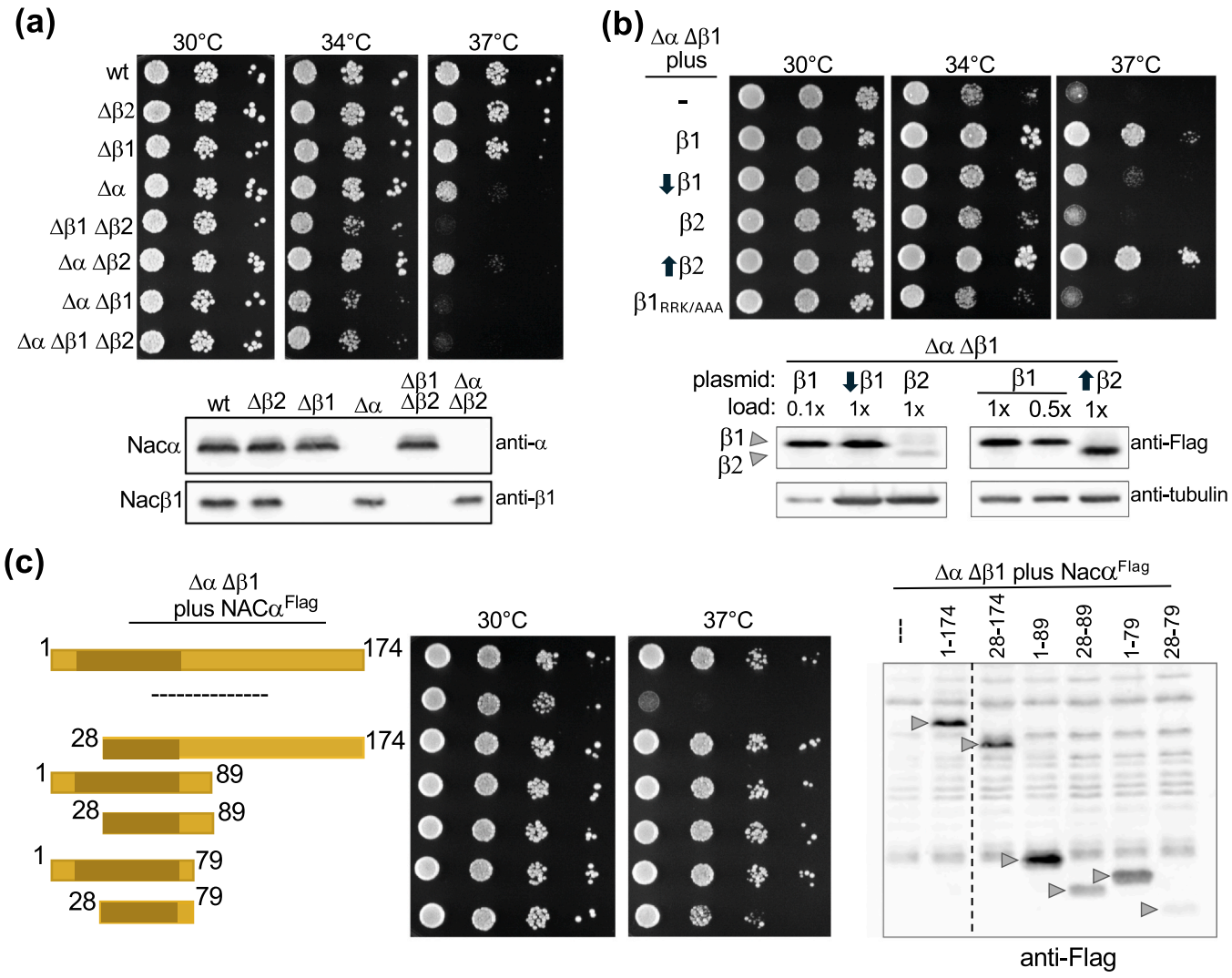

Fig. 6 Growth defects when Nacα is absent. (a) Top. Growth of wild-type (WT) and strains with indicated deletions of genes encoding NAC subunits: Nacα (Δα), Nacβ1 (Δβ1), Nacβ2 (Δβ2), or combinations. Ten-fold serial dilutions were plated and incubated at indicated temperatures for 2 days. Bottom. Immunoblot analysis of cell extracts, from indicated deletion strains, after separation by SDS-PAGE, using antibody specific for Nacα or Nacβ1. (b) Requirement of a beta NAC when Nacα is absent. Top. Ten-fold serial dilutions of Δ*nac*α Δ*nac*β1 (Δα Δβ1) cells transformed with plasmids expressing the indicated NAC proteins having a Flag tag were plated and incubated at indicated temperatures for 2 days. Empty vector (-); Nacβ2 promoter driving expression of Nacβ1 (↓β1); the strong *ADH1* promoter driving Nacβ2 (↑β2). Bottom. The indicated amount of cell lysates (load) from Δα Δβ1 cells containing a plasmid expressing the indicated Flag-tagged NAC subunit were subjected to immunoblot analysis using Flag or, as a control, tubulin-specific antibodies. (c) Nacα truncations. Left. Ten-fold serial dilutions of Δ*nac*α Δ*nac*β1 (Δα Δβ1) cells transformed with a plasmid expressing the indicated Nacα deletion variants having a Flag tag or empty vector (—) were plated and incubated at the indicated temperatures for two days. Right. Immunoblot analysis of cell extracts of indicated deletion strains separated by SDS-PAGE using antibody specific for Flag tag. Nacα fragments are indicated by arrowheads. The dotted line indicates that an irrelevant lane of the gel was cropped out of the immunoblot image. (d) Lowered Nacα expression. Left. Ten-fold serial dilutions of Δ*nac*α Δ*nac*β (Δα Δβ1) cells transformed with plasmids were plated and incubated at the indicated temperatures for 2 days (30 or 34 °C) or 3 days (37 °C). Nacα under its native promoter, α; Nacα under the Nacβ2 promoter, ↓α; empty vector, -. Right. Immunoblot analysis of lysates from wt and Δα Δβ1 cells expressing Nacα driven by the Nacβ2 promoter (↓α).

We, therefore, compared all combinations of NAC deletions. Of the three double deletion strains, two grew very poorly at 37 ° and more slowly than WT cells at 34 °C −Δ*nac*α Δ*nac*β1 and Δ*nac*β1 Δ*nac*β2, which was discussed above. The triple deletion Δ*nac*α Δ*nac*β1 Δ*nac*β2 grew similarly to these two double mutants (Figure 6(a)).

The relatively robust growth of cells expressing Nacβ1 in the absence of Nacα suggests that Nacβ1 is able to, at least to some extent, act independently of Nacα. In other words, a heterodimer is not absolutely required for all NAC-related activity. This result raises the question of whether Nacβ2 could suffice in place of Nacβ1 if present in sufficient amounts. We therefore placed Nacβ2 under the control of the *ADH1* promoter, which drove its expression to approximately the same level as that of NACβ1 (Figure 6(b)). This construct was able to rescue the temperature-sensitive growth defect caused by the lack of Nacα and Nacβ1 (Figure 6(b)). The previously described construct having Nacβ1 driven by the Nacβ2 promoter, and therefore expressing lower amounts of Nacβ1, did not rescue growth nearly as well as a construct expressing Nacβ1 from its native promoter.

Together these results indicate that, for the function (s) successfully carried out in the absence of Nacα, either Nacβ1 or Nacβ2 suffices—as long as expression is high. They are also consistent with previous indications that beta subunits may well function as homodimers.[8,43] Whether the requirement for high expression is because only a small amount of functional homodimer is formed or that the sequences in Nacα possess activity important for this function is not clear. Interestingly, Nacβ1 having the RRK/AAA mutation Nacβ1$_{RRK/AAA}$ was not able to rescue the temperature-sensitive phenotype of cells lacking Nacα (Figure 6(b)). Whether this is because Nacα substantially affects ribosome association, partially overcoming the effects of the RRK/AAA mutation remains an open question. It should be noted that the Nacα alpha helix in the globular domain of metazoan NAC has been implicated in ribosome association.[42]

We next made truncation mutants to test if N or C terminal sequences of Nacα are important for cell growth in the absence of Nacβ1. Deletions removing N-terminal or C-terminal segments that included the ubiquitin association domain supported growth as well as full-length protein (Figure 6(c)). Even a 51 residue 28–79 fragment supported colony formation at 37 °C, though growth was not as robust as when other constructs were used. However, its level of expression was much lower than that of other constructs (Figure 6(c)). We therefore wanted to ask if lower expression of full-length Nacα sufficed. Nacα was placed under the control of the Nacβ2 promoter. Lower levels of Nacα were sufficient to support robust growth (Figure 6(d)). Together, our results suggest that only the core domain of Nacα suffices to overcome the growth defect of strains expressing only low levels of the beta subunit, that is NACβ2. This limited requirement is consistent with the possibility that for this phenotype the important function of the alpha subunit is to efficiently form dimers, maintaining the beta subunit in a functional conformation.

Concluding remarks

Our results from combining experimental and evolutionary analyses are consistent with the following scenario regarding the regulatory interaction of Nacβ2 with the Caf130 subunit of the CCR4–Not complex: Caf130 emerged prior to the WGD. After the WGD, Nacβ2 of the Saccharomyces lineage underwent extensive divergence. Among the amino acid substitutions, two outside the globular domain were necessary for Nacβ2′s interaction with Caf130. As described previously,[16] this positions the CCR4–Not complex such that Rpl4 mRNA is degraded in the absence of its specific chaperone, Acl4.

Our results also indicate that it may be more difficult than generally appreciated to completely disrupt NAC binding to the ribosome without mutating sequences that have other functions. This makes it challenging to formulate definitive conclusions about the relationship between ribosome association and function and also highlights the need for methods to assess associations within the cell, as well as *in vitro* biochemical and structural approaches.

In a broader context, it should be emphasized that *S. cerevisiae* has an unusually complex system of factors at the ribosome tunnel exit—not only the two beta NAC subunits found only in closely related yeast species, the subject of this report, but also the complex tripartite Hsp70 system found in all fungi, including a ribosome-specific Hsp70. Likely because of this, the apparent phenotypes observed upon disruption of NAC in *S. cerevisiae* are not dramatic compared to those seen in metazoans. Yet, as analyses become more nuanced, more phenotypes are becoming more apparent. One example is the Acl4-related phenotype exploited here. But it also has been recently shown that Nacβ1 and Nacβ2 play roles in other important cellular processes—in selective mitochondrial degradation[44] and mitochondrial protein import,[45] respectively. Future research will likely uncover additional roles.

Materials and methods

Evolutionary analyses

Orthologs of Nacβ1 and Nacβ2 sequences were retrieved from OMA orthology database HOG_B0614165 group,

KEGG, and Yeast Protein Database (YPD). Nacβ1 and Nacβ2 orthologs in post-WGD species were identified using synteny viewer at Yeast Genome Order Browser. Sequences were aligned using Clustal Omega v1.2.2 with default parameters. Alignment logos were generated using the WebLogo3 server.[46] Protein phylogeny, with constrained topology such that Nacβ2 and Nacβ1 share common ancestry at the node representing WGD, was inferred using the maximum likelihood method (ML). One thousand ML searches were performed using iQ-TREE[47] with 1000 rapid bootstrap replicates, under the LG model of amino acid substitution and GAMMA model of rate heterogeneity with four discrete rate categories and the estimate of the proportion of invariable sites (LG + I + F +G4),[48] which was determined as the best-fit model by Bayesian Information Criterion with ModelFinder.[49] The constrained tree was validated against unconstrained tree topology using approximately unbiased test[50] with P-value > 0.05. To map amino acid substitutions that took place on the branches leading to Nacβ2 and Nacβ1 of Saccharomyces species, sequences at the nodes connected by these branches were compared. These sequences were inferred based on the phylogeny ancestral sequences reconstruction method using the FastML program based on the ML algorithm for insertions and deletions reconstruction and the Empirical Bayes method using the LG substitution matrix with gamma parameter.[51] Structural visualizations used Blender (https://www.blender.org/).

Strains and plasmids

Saccharomyces cerevisiae strains and plasmids used in this study are listed in Tables S1 and Table S2, respectively. Integrated DNA Technologies (Coraville, IA) was used for the synthesis of all primers and gBlocks. Codon substitutions, deletions, and insertion mutations were introduced into cloned DNA using the QuikChange protocol (Stratagene, La Jolla, CA). Genomic DNA was isolated using the MasterPure™ yeast DNA purification kit from Lucigen (Middleton, WI). All plasmid constructs underwent sequence analysis by Functional Biosciences (Madison, WI). Yeast was grown in either rich media, YPD (1% yeast extract, 2% peptone [Difco Laboratories, Detroit, MI], 2% dextrose) or selective minimal media (0.67% yeast nitrogen base without amino acids [US Biological, Marblehead, MA], 2% dextrose) supplemented with required amino acids.[52] All plates shown in this report are minimal media unless stated otherwise. DNA was transformed into yeast using a previously published protocol.[53] Cell growth assays were performed by serially diluting cells for each strain in 10-fold increments starting with 5000 cells in the first position and spotting on plates.

Deletions of genes encoding NAC subunits α (*EGD2*) and β1 (*EGD1*) were created in the W303 yeast strain background[54] by CRISPR, as previously described.[15] The gene encoding Nacβ2 (*BTT1*) was similarly deleted using CRISPR. Specifically, a target-specific single-guide RNA (sgRNA) was constructed by cloning a 60-mer bridging primer, which contains a 20-nucleotide target sequence of +385 to +404 for *BTT1*, into *Not*I-digested pXIPHOS vector (accession MG897154, GenBank) using NEBuilder HiFi DNA assembly Master Mix (New England Biolabs). A *BTT1*-specific gBlock was synthesized containing 216 bp of DNA upstream of the ATG and 226 bp of DNA downstream of the stop codon to serve as rescue DNA. The XIPHOS-*BTT1* sgRNA plasmid, along with a 20-fold molar excess of rescue DNA, was transformed into yeast, and deletion candidates were selected for on YPD containing 100 μg/mL of nourseothricin (Werner BioAgents GmbH, Jena, Germany). Resistant colonies were tested using colony PCR with primers that bind within the upstream and downstream untranslated regions of *BTT1*. A 3x-Flag tag was introduced at the 3′ end of *BTT1*′s ORF using CRISPR. The same sgRNA plasmid was used to transform the desired yeast strain along with a gBlock containing 157 bp upstream of the stop codon, a 66 bp flag tag, and 190 bp downstream of the stop codon. The sequence at the target site in the rescue DNA was altered, resulting in a glycine to alanine change at residue 136. Correct addition of the flag tag sequence was confirmed first by colony PCR of nourseothricin-resistant colonies and observing a size increase compared to WT, and second, by sequencing the PCR-generated fragments of the correct size.

To delete *ACL4* by homologous recombination in the W303 background, a DNA fragment containing a KanMX cassette replacement of the *ACL4* ORF was amplified from genomic DNA isolated from the deletion library[55] by PCR and transformed into the desired yeast strain. Deletion candidates, which grew on YPD with 200 μg/mL G418 sulfate (VWR Chemicals, LLC Sanbom, NY), were tested by colony PCR with primers specific to KanMX and to the UTR of *ACL4*.

The *BTT1* gene encoding Nacβ2, with a Flag tag, was cloned by amplifying genomic DNA from the strain containing the integrated Flag tag with primers that introduce a *Bam*HI site at the 5′ end (at the ATG or 200 bp upstream) and an *Xho*I site at the 3′ end (240 bp downstream of stop codon). After restriction digestion of the PCR products, the DNA was ligated into similarly digested plasmid DNAs: pRS314[56] and p414ADH.[57] *EGD1* (Nacβ1) and *EGD2* (Nacα) were cloned into

pRS314 and pRS316, respectively, by PCR amplifying the genes from genomic DNA using primers that contain a *Bam*HI site at the 5′ end (371 and 344 bp upstream of ATG, respectively) and an *Xho*I site at the 3′ end (246 and 239 bp downstream of the stop codon, respectively). A 3x-Flag tag was added to the C-terminus of both Egd1 and Egd2 by subcloning in gBlocks containing the tag sequence using *Hin*dIII-*Xho*I for *EGD1* and *Bgl*II-*Xho*I for *EGD2*. In order to lower the expression of Egd1 and Egd2, their ORFs were cloned as *Bam*HI-*Xho*I fragments into p414ADH and p416ADH, respectively, in which the *ADH1* promoter was replaced with −200 to −1 of *BTT1*'s 5′ UTR. The complete ORF of Caf130 was cloned into the two-hybrid plasmid pGAD-C1[58] as a *Bam*HI-*Sal*I digested PCR fragment. *BTT1* and *EGD1*, full-length and variants, were cloned into pGBD-C1 as *Bam*HI-*Sal*I digested PCR fragments.

Immunoblot analysis and site-specific crosslinking

To make whole cell lysates, yeast cells were harvested in log-phase growth (OD_{600} 0.8–1.0), treated with 0.2 N NaOH for 5 min, resuspended in sample buffer, and boiled for 5 min[59] Samples were resolved on sodium dodecyl sulfate polyacrylamide gel using BLUeye-prestained markers (Sigma-Aldrich, St. Loius, MO), transferred electrophoretically to nitrocellulose, and subjected to immunoblot analysis using the Enhanced Chemi-Luminescence System (GE Healthcare) according to the manufacturer's suggestion. Antitubulin (12G10) and Rpl3 (ScRPL3) antibodies were obtained from the monoclonal antibody facility at the University of Iowa (University Heights, IA). Anti-FLAG monoclonal M2 antibody came from Sigma-Aldrich (St. Louis, MO). Antibodies specific for Egd1 (Nacβ1), Egd2 (Nacα),[15] and Ssb[60] were previously described.

In vivo crosslinking was carried out as described previously.[15] The Δ*ssb1* Δ*ssb2* Δ*nac*β1 strain was transformed with plasmids able to express $Ssb1^{S563TAG}$ and the indicated $Nac\beta1^{Flag}$ construct, as well as a plasmid carrying a suppressor transfer RNA to direct incorporation of p-benzoyl-L-phenylalanine (Bpa) at the TAG stop codon. Log-phase cultures were treated with cycloheximide (0.1 mg/mL final) and exposed to UV light to induce crosslinking prior to glass bead lysis. Cells were lysed by agitation with glass beads for 5 × 1 min (with 1 min on ice between) at 4 °C in lysis buffer (300 mM sorbitol, 20 mM HEPES-KOH, pH 7.5, 1 mM EGTA, 5 mM $MgCl_2$, 10 mM KCl, 10% glycerol v/v, 1 mM dithiothreitol, and RNasin RNase Inhibitor [Promega]) at a dilution of 1:1000. Lysates were clarified by centrifugation at 16,100 rcf for 10 min in a microcentrifuge (Eppendorf). A 4 Abs_{260} units of each lysate were applied to a 0.4 mL sucrose cushion in which 0.5 M sucrose replaced 0.3 M sorbitol in the lysis buffer. Samples were centrifuged for 105 min at 108 900 relative centrifugal force in a TLA120.1 rotor (Beckman Coulter) at 4 °C. A 0.15 mL was subsequently removed from the top of the tube to yield the soluble fraction. The ribosomal pellet was resuspended in sample buffer, and 12.5% SDS-PAGE gels were loaded with equivalent portions of lysate (equivalent to 0.2 Abs260 units/lane of starting extract), soluble, and pellet fractions.

Funding and support This study was supported by grants from the National Institutes of Health (R35 GM127009 to E.A.C.) and the National Science Center, Poland (OPUS 21 2021/41/B/NZ8/02835 to B.T.).

Author contributions **Elizabeth Craig:** Writing – review & editing, Writing – original draft, Funding acquisition, Conceptualization. **Bartlomiej Tomiczek:** Writing – review & editing, Investigation, Funding acquisition. **Jaroslaw Marszalek:** Writing – review & editing, Writing – original draft, Conceptualization. **Przemyslaw Domanski** and **Thomas Ziegelhoffer:** Writing – review & editing, Investigation. **Brenda A Schilke:** Writing – review & editing, Investigation, Conceptualization.

Data availability statement Data will be made available on request.

Declarations of interest The authors declare that they have no known competing financial interests or personal relationships that could have appeared to influence the work reported in this paper.

Acknowledgments We thank Amit K. Verma and Wojciech Delewski for the construction of some of the plasmids and strains used in this study. We also thank Marcin Pitek for his helpful and insightful insights into protein structures.

Appendix A. Supplementary Data

Supplementary data associated with this article can be found in the online version at doi:10.1016/j.cstres.2024.10.004.

References

1. Gamerdinger M, Deuerling E. Cotranslational sorting and processing of newly synthesized proteins in eukaryotes. *Trends Biochem Sci.* 2024;49:105–118. https://doi.org/10.1016/j.tibs.2023.10.003
2. Wiedmann B, Sakai H, Davis TA, Wiedmann M. A protein complex required for signal-sequence-specific sorting and translocation. *Nature.* 1994;370:434–440. https://doi.org/10.1038/370434a0
3. Hsieh HH, Shan SO. Fidelity of cotranslational protein targeting to the endoplasmic reticulum. *Int J Mol Sci.* 2021;23:281. https://doi.org/10.3390/ijms23010281
4. Shen K, Gamerdinger M, Chan R, et al. Dual role of ribosome-binding domain of NAC as a potent suppressor of protein aggregation and aging-related proteinopathies. *Mol*

Cell. 2019;74:729–741.e727. https://doi.org/10.1016/j.molcel.2019.03.012
5. Wang L, Zhang W, Wang L, Zhang XC, Li X, Rao Z. Crystal structures of NAC domains of human nascent polypeptide-associated complex (NAC) and its alphaNAC subunit. *Protein Cell.* 2010;1:406–416. https://doi.org/10.1007/s13238-010-0049-3
6. Liu Y, Hu Y, Li X, Niu L, Teng M. The crystal structure of the human nascent polypeptide-associated complex domain reveals a nucleic acid-binding region on the NACA subunit. *Biochemistry.* 2010;49:2890–2896. https://doi.org/10.1021/bi902050p
7. Wegrzyn RD, Hofmann D, Merz F, et al. A conserved motif is prerequisite for the interaction of NAC with ribosomal protein L23 and nascent chains. *J Biol Chem.* 2006;281:2847–2857. https://doi.org/10.1074/jbc.M511420200
8. Pech M, Spreter T, Beckmann R, Beatrix B. Dual binding mode of the nascent polypeptide-associated complex reveals a novel universal adapter site on the ribosome. *J Biol Chem.* 2010;285:19679–19687. https://doi.org/10.1074/jbc.M109.092536
9. Hu GZ, Ronne H. Yeast BTF3 protein is encoded by duplicated genes and inhibits the expression of some genes in vivo. *Nucleic Acids Res.* 1994;22:2740–2743. https://doi.org/10.1093/nar/22.14.2740
10. Reimann B, Bradsher J, Franke J, et al. Initial characterization of the nascent polypeptide-associated complex in yeast. *Yeast* . 1999;15:397–407. https://doi.org/10.1002/(SICI)1097-0061(19990330)15:5<397::AID-YEA384>3.0.CO;2-U
11. Wong ED, Miyasato SR, Aleksander S, et al. Saccharomyces genome database update: server architecture, pan-genome nomenclature, and external resources. *Genetics.* 2023;224:14. https://doi.org/10.1093/genetics/iyac191
12. Rospert S, Dubaquie Y, Gautschi M. Nascent-polypeptide-associated complex. *Cell Mol Life Sci.* 2002;59:1632–1639. https://doi.org/10.1007/pl00012490
13. Ott AK, Locher L, Koch M, Deuerling E. Functional dissection of the nascent polypeptide-associated complex in *Saccharomyces cerevisiae*. *PLoS One.* 2015;10:e0143457. https://doi.org/10.1371/journal.pone.0143457
14. Koplin A, Preissler S, Ilina Y, et al. A dual function for chaperones SSB-RAC and the NAC nascent polypeptide-associated complex on ribosomes. *J Cell Biol.* 2010;189:57–68. https://doi.org/10.1083/jcb.200910074
15. Ziegelhoffer T, Verma AK, Delewski W, et al. NAC and Zuotin/Hsp70 chaperone systems coexist at the ribosome tunnel exit in vivo. *Nucleic Acids Res.* 2024;52:3346–3357. https://doi.org/10.1093/nar/gkae005
16. Pillet B, Mendez-Godoy A, Murat G, et al. Dedicated chaperones coordinate co-translational regulation of ribosomal protein production with ribosome assembly to preserve proteostasis. *Elife.* 2022;11. https://doi.org/10.7554/eLife.74255
17. Pillet B, Garcia-Gomez JJ, Pausch P, et al. The dedicated chaperone Acl4 escorts ribosomal protein Rpl4 to its nuclear Pre-60S assembly site. *PLoS Genet.* 2015;11:43. https://doi.org/10.1371/journal.pgen.1005565
18. Stelter P, Huber FM, Kunze R, Flemming D, Hoelz A, Hurt E. Coordinated ribosomal L4 protein assembly into the pre-ribosome is regulated by its eukaryote-specific extension. *Mol Cell.* 2015;58:854–862. https://doi.org/10.1016/j.molcel.2015.03.029
19. Laribee RN. Ccr4-Not as a mediator of environmental signaling: a jack of all trades and master of all. *Curr Genet.* 2021;67:707–713. https://doi.org/10.1007/s00294-021-01180-5
20. Morris C, Cluet D, Ricci EP. Ribosome dynamics and mRNA turnover, a complex relationship under constant cellular scrutiny. *Wiley Interdiscip Rev RNA.* 2021;12:e1658. https://doi.org/10.1002/wrna.1658
21. Collart MA, Audebert L, Bushell M. Roles of the CCR4-Not complex in translation and dynamics of co-translation events Wiley Interdiscip Rev RNA. 2023;15:e1827. https://doi.org/10.1002/wrna.1827
22. Jakel S, Mingot JM, Schwarzmaier P, Hartmann E, Gorlich D. Importins fulfil a dual function as nuclear import receptors and cytoplasmic chaperones for exposed basic domains. *EMBO J.* 2002;21:377–386. https://doi.org/10.1093/emboj/21.3.377
23. Cui Y, Ramnarain DB, Chiang YC, Ding LH, McMahon JS, Denis CL. Genome wide expression analysis of the CCR4-NOT complex indicates that it consists of three modules with the NOT module controlling SAGA-responsive genes. *Mol Genet Genomics.* 2008;279:323–337. https://doi.org/10.1007/s00438-007-0314-1
24. Wolfe KH, Shields DC. Molecular evidence for an ancient duplication of the entire yeast genome. *Nature.* 1997;387:708–713. https://doi.org/10.1038/42711
25. Kellis M, Birren BW, Lander ES. Proof and evolutionary analysis of ancient genome duplication in the yeast *Saccharomyces cerevisiae*. *Nature.* 2004;428:617–624. https://doi.org/10.1038/nature02424
26. Wagner A. Asymmetric functional divergence of duplicate genes in yeast. *Mol Biol Evol.* 2002;19:1760–1768. https://doi.org/10.1093/oxfordjournals.molbev.a003998
27. Gu X, Zhang Z, Huang W. Rapid evolution of expression and regulatory divergences after yeast gene duplication. *Proc Natl Acad Sci USA.* 2005;102:707–712. https://doi.org/10.1073/pnas.0409186102
28. Kim SH, Yi SV. Correlated asymmetry of sequence and functional divergence between duplicate proteins of *Saccharomyces cerevisiae*. *Mol Biol Evol.* 2006;23:1068–1075. https://doi.org/10.1093/molbev/msj115
29. Soria PS, McGary KL, Rokas A. Functional divergence for every paralog. *Mol Biol Evol.* 2014;31:984–992. https://doi.org/10.1093/molbev/msu050
30. Kuzmin E, VanderSluis B, Nguyen Ba AN, et al. Exploring whole-genome duplicate gene retention with complex genetic interaction analysis. *Science.* 2020;368. https://doi.org/10.1126/science.aaz5667
31. Pal C, Papp B, Hurst LD. Highly expressed genes in yeast evolve slowly. *Genetics.* 2001;158:927–931. https://doi.org/10.1093/genetics/158.2.927
32. Drummond DA, Bloom JD, Adami C, Wilke CO, Arnold FH. Why highly expressed proteins evolve slowly. *Proc Natl Acad Sci USA.* 2005;102:14338–14343. https://doi.org/10.1073/pnas.0504070102
33. Drummond DA, Raval A, Wilke CO. A single determinant dominates the rate of yeast protein evolution. *Mol Biol Evol.* 2006;23:327–337. https://doi.org/10.1093/molbev/msj038
34. Humphreys IR, Pei J, Baek M, et al. Computed structures of core eukaryotic protein complexes. *Science.* 2021;374:eabm4805. https://doi.org/10.1126/science.abm4805
35. Gamerdinger M, Jia M, Schloemer R, et al. NAC controls co-translational N-terminal methionine excision in eukaryotes. *Science.* 2023;380:1238–1243. https://doi.org/10.1126/science.adg3297
36. Gamerdinger M, Kobayashi K, Wallisch A, et al. Early scanning of nascent polypeptides inside the ribosomal tunnel by NAC. *Mol Cell.* 2019;75:996–1006.e1008. https://doi.org/10.1016/j.molcel.2019.06.030
37. Panasenko O, Landrieux E, Feuermann M, Finka A, Paquet N, Collart MA. The yeast Ccr4-Not complex controls

ubiquitination of the nascent-associated polypeptide (NAC-EGD) complex. *J Biol Chem.* 2006;281:31389–31398. https://doi.org/10.1074/jbc.M604986200
38. Alhusaini N, Coller J. The deadenylase components Not2p, Not3p, and Not5p promote mRNA decapping. *RNA.* 2016;22:709–721. https://doi.org/10.1261/rna.054742.115
39. Deuerling E, Gamerdinger M, Kreft SG. Chaperone interactions at the ribosome. *Cold Spring Harb Perspect Biol.* 2019;11:a033977. https://doi.org/10.1101/cshperspect.a033977
40. Hsieh HH, Lee JH, Chandrasekar S, Shan SO. A ribosome-associated chaperone enables substrate triage in a cotranslational protein targeting complex. *Nat Commun.* 2020;11:5840. https://doi.org/10.1038/s41467-020-19548-5
41. Jomaa A, Gamerdinger M, Hsieh HH, et al. Mechanism of signal sequence handover from NAC to SRP on ribosomes during ER-protein targeting. *Science.* 2022;375:839–844. https://doi.org/10.1126/science.abl6459
42. Muthukumar G, Stevens TA, Inglis AJ, et al. Triaging of alpha-helical proteins to the mitochondrial outer membrane by distinct chaperone machinery based on substrate topology. *Mol Cell.* 2024;84:1101–1119.e1109. https://doi.org/10.1016/j.molcel.2024.01.028
43. del Alamo M, Hogan DJ, Pechmann S, Albanese V, Brown PO, Frydman J. Defining the specificity of cotranslationally acting chaperones by systematic analysis of mRNAs associated with ribosome-nascent chain complexes. *PLoS Biol.* 2011;9:e1001100. https://doi.org/10.1371/journal.pbio.1001100
44. Tian Y, Okamoto K. The nascent polypeptide-associated complex subunit Egd1 is required for efficient selective mitochondrial degradation in budding yeast. *Sci Rep.* 2024;14:546. https://doi.org/10.1038/s41598-023-50245-7
45. Avendano-Monsalve MC, Mendoza-Martinez AE, Ponce-Rojas JC, Poot-Hernandez AC, Rincon-Heredia R, Funes S. Positively charged amino acids at the N terminus of select mitochondrial proteins mediate early recognition by import proteins alphabeta'-NAC and Sam37. *J Biol Chem.* 2022;298:10. https://doi.org/10.1016/j.jbc.2022.101984
46. Crooks GE, Hon G, Chandonia JM, Brenner SE. WebLogo: a sequence logo generator. *Genome Res.* 2004;14:1188–1190. https://doi.org/10.1101/gr.849004
47. Nguyen LT, Schmidt HA, von Haeseler A, Minh BQ. IQ-TREE: a fast and effective stochastic algorithm for estimating maximum-likelihood phylogenies. *Mol Biol Evol.* 2015;32:268–274. https://doi.org/10.1093/molbev/msu300
48. Le SQ, Gascuel O. An improved general amino acid replacement matrix. *Mol Biol Evol.* 2008;25:1307–1320. https://doi.org/10.1093/molbev/msn067
49. Kalyaanamoorthy S, Minh BQ, Wong TKF, von Haeseler A, Jermiin LS. ModelFinder: fast model selection for accurate phylogenetic estimates. *Nat Methods.* 2017;14:587–589. https://doi.org/10.1038/nmeth.4285
50. Shimodaira H. An approximately unbiased test of phylogenetic tree selection. *Syst Biol.* 2002;51:492–508. https://doi.org/10.1080/10635150290069913
51. Ashkenazy H, Penn O, Doron-Faigenboim A, et al. FastML: a web server for probabilistic reconstruction of ancestral sequences. *Nucleic Acids Res.* 2012;40:W580–W584. https://doi.org/10.1093/nar/gks498
52. Sherman F, Fink G, Hicks J. *Methods in Yeast Genetics.* 500 Sunnyside Boulevard, Woodbury, NY: Cold Spring Harbor Press; 1986.11797-2924.
53. Chen DC, Yang BC, Kuo TT. One-step transformation of yeast in stationary phase. *Curr Genet.* 1992;21:83–84. https://doi.org/10.1007/BF00318659
54. Thomas BJ, Rothstein R. Elevated recombination rates in transcriptionally active. *DNA Cell.* 1989;56:619–630. https://doi.org/10.1016/0092-8674(89)90584-9
55. Giaever G, Chu AM, Ni L, et al. Functional profiling of the *Saccharomyces cerevisiae* genome. *Nature.* 2002;418:387–391. https://doi.org/10.1038/nature00935
56. Sikorski RS, Hieter P. A system of shuttle vectors and yeast host strains designed for efficient manipulation of DNA in *Saccharomyces cerevisiae*. *Genetics.* 1989;122:19–27. https://doi.org/10.1093/genetics/122.1.19
57. Mumberg D, Muller R, Funk M. Yeast vectors for the controlled expression of heterologous proteins in different genetic backgrounds. *Gene.* 1995;156:119–122. https://doi.org/10.1016/0378-1119(95)00037-7
58. James P, Halladay J, Craig EA. Genomic libraries and a host strain designed for highly efficient two-hybrid selection in yeast. *Genetics.* 1996;144:1425–1436. https://doi.org/10.1093/genetics/144.4.1425
59. Kushnirov VV. Rapid and reliable protein extraction from yeast. *Yeast.* 2000;16:857–860. https://doi.org/10.1002/1097-0061(20000630)16:9<857::AID-YEA561>3.0.CO;2-B
60. Lopez-Buesa P, Pfund C, Craig EA. The biochemical properties of the ATPase activity of a 70-kDa heat shock protein (Hsp70) are governed by the C-terminal domains. *Proc Natl Acad Sci USA.* 1998;95:15253–15258. https://doi.org/10.1073/pnas.95.26.15253